SEARCHING TO EXPLOIT MEMORIZATION EFFECT IN LEARNING FROM CORRUPTED LABELS

Anonymous authors
Paper under double-blind review

ABSTRACT

Sample-selection approaches, which attempt to pick up clean instances from the noisy training data set, have become one promising direction to robust learning from corrupted labels. These methods all build on the memorization effect, which means deep networks learn easy patterns first and then gradually over-fit the training data set. In this paper, we show how to properly select instances so that the training process can benefit the most from the memorization effect is a hard problem. Specifically, memorization can heavily depend on many factors, e.g., data set and network architecture. Nonetheless, there still exists general patterns of how memorization can occur. These facts motivate us to exploit memorization by automated machine learning (AutoML) techniques. First, we design an expressive but compact search space based on observed general patterns. Then, we propose to use the natural gradient-based search algorithm to efficiently search through space. Finally, extensive experiments on both synthetic data sets and benchmark data sets demonstrate that the proposed method can not only be much efficient than existing AutoML algorithms but can also achieve much better performance than the state-of-the-art approaches for learning from corrupted labels.

1 INTRODUCTION

Learning with deep neural networks has enjoyed huge empirical success in recent years across a wide variety of tasks, from image processing to speech recognition, and from language modeling to recommender system (Goodfellow et al., 2016). However, their success highly counts on the availability of well-annotated and big data, which is barely available for real-world applications. Instead, what we are facing with in practice are large data sets which are collected from crowd-sourcing platforms or crawled from the Internet, thus containing many corrupted labels (Li et al., 2017b; Patrini et al., 2017). Besides, due to the vast learning capacity of deep networks, they will eventually over-fit on these corrupted labels, leading to poor predicting performance, which can be worse than that obtained from simple models (Zhang et al., 2016; Arpit et al., 2017).

To reduce the negative effect of corrupted labels, many methods have been proposed. Sukhbaatar et al. (2015); Patrini et al. (2017) focus on estimating on the noise transition matrix. However, the noise transition matrix can be hard to accurately estimate, especially when the number of classes is large (Han et al., 2018). To be free of estimating the noise transition matrix, a promising direction is training networks only on *selected instances* that are more likely to be clean (Jiang et al., 2018; Han et al., 2018; Ma et al., 2018; Yu et al., 2019). Intuitively, as the training data becomes less noisy, better performance can be obtained. Among those works, the representative methods are MentorNet (Jiang et al., 2018) and Co-teaching (Han et al., 2018; Yu et al., 2019). Specifically, MentorNet pre-trains an extra network, and then uses the extra network for selecting clean instances to guide the training. When the clean validation data is not available, MentorNet has to use a predefined curriculum (Bengio et al., 2009). Co-teaching maintains two networks which have identical architectures simultaneously during the training process. And in each mini-batch of data, each network is updated using *the other* network's small-loss instances. Empirical results demonstrate that under both extremely and low-level noise, Co-teaching can achieve much better performance than MentorNet.

To the success of these sample-selection methods, the memorization effect of deep networks (Zhang et al., 2016; Arpit et al., 2017) is the crux. Memorization happens widely in various architectures of deep network, e.g., multilayer perceptron (MLP) and convolutional neural network (CNN). They all tend to learn easy patterns first and then over-fit on (possibly noisy) training data set. Due to such effect, sample-selection methods can learn correct patterns at early stage and then use the obtained discriminative ability to filter out corrupted instances in subsequent training epochs (Han et al., 2018; Chen et al., 2019). However, these methods are hard to tune with good performance. The problem is that it is difficult to exactly control how many instances need to be filtered out during different stages in the training; and trivial attempts can easily lead to even worse performance than standard deep networks (Han et al., 2018). Some recent endeavors seek to evade from this problems by integrating with other auxiliary information, e.g., a small clean subset is used in (Ren et al., 2018), and knowledge graphs are utilized in (Li et al., 2017b).

In this paper, motivated by the success of automated machine learning (AutoML) on designing data-dependent models (Hutter et al., 2018), we propose to exploit memorization effects automatically using AutoML techniques. Contributions are summarized as follows:

- First, to have an in-depth understanding of why it is difficult to exploit the memorization effect, we examine its behaviors from the perspective of practical usage. We find that, while there exist general patterns in how memorization occurs with the training process, it is hard to quantize to which extend such effect can happen. Especially, memorization can be affected by many factors, e.g., data sets used, noisy types, network architectures, and the choice of the optimizers.
- To make good use of AutoML techniques, we then derive an expressive search space for exploiting memorization, which is from the above observations, i.e., the curvature of how many instances need to be sampled during iterating should be similar with the inverse of the learning curve on the validation set. Such a space is not too huge since it has only a few variables, thus allows subsequent algorithms converging fast to promising candidates. Besides, it is also not too small, as it covers all necessary functions, i.e., not just a specific function used in the past but also many functions can be considered in the future.
- Then, to design an efficient algorithm, we first show the difficulty of getting gradients in our space and the failure of weight-sharing with the existence of corrupted labels. These motivate us to take a probabilistic view of the search problem and adopt natural gradient descent (Amari, 1998; Pascanu & Bengio, 2013) for optimization. The designed algorithm can effectively address above problems and is significantly faster than other popular search algorithms.
- Finally, we conduct extensive experiments on both synthetic and benchmark data sets, under various settings using different network architectures. These experiments demonstrate that the proposed method can not only be much more efficient than existing AutoML algorithms, but also can achieve much better performance than the state-of-the-art sample-selection approaches designed by humans. Besides, we further visualize and explain the searched functions, which can also help design better rules to control memorization effects in the future.

2 Related work

2.1 Learning from Noisy Labels

The mainstream research focuses on *class-conditional noise* (CCN) (Angluin & Laird, 1988), where the label corruption is independent of features. Generally, recent methods for handling CCN model can be classified into three categories. The first one is based on the estimation of transition matrix, which tries to capture how correct labels flip into wrong ones (Sukhbaatar et al., 2015; Reed et al., 2015; Patrini et al., 2017; Ghosh et al., 2017). These methods then use the estimated matrix to correct gradients or loss during training. However, they are fragile to heavy noise and unable to handle many classes (Han et al., 2018). The second type is the regularization approach (Miyato et al., 2016; Laine & Aila, 2017; Tarvainen & Valpola, 2017). Although regularization approach can achieve a satisfying performance, it is still an *incomplete* approach since (Jiang et al., 2018) shows that it can only *delay* the overfitting progress rather than *avoid* it, i.e. given enough training time, it can still fit the noisy data completely. Thus, it requires much domain knowledge to determine the appropriate number of training epochs in order to prevent overfitting. The last one is sample-selection approach, which attempts to reduce negative effects from noisy labels by selecting clean instances during training. The recent state-of-the-art method is also built on sample-selection approach (Jiang et al., 2018; Han et al., 2018; Malach & Shalev-Shwartz, 2017; Yu et al., 2019).

A promising criteria to select "clean instances" is to pick up instances that has relatively small losses in each mini-batch (Jiang et al., 2018; Han et al., 2018). The fundamental property behind these methods is the memorization effect of deep networks (Zhang et al., 2016; Arpit et al., 2017), which means deep networks can learn simple patterns first and then start to over-fit. Such effect helps classifiers set up discriminate ability in the early stage, then make clean instances more likely to have smaller loss that those corrupted ones. The general framework of sample-selection approach is in Algorithm 1. Specifically, some small-loss instances $\bar{\mathcal{D}}_f$ are selected from the mini-batch $\bar{\mathcal{D}}$ in step 5. These "clean" instances are then used to update network parameters in step 6. The $R(t)$ in step 8, which controls how many instances to be kept in each epoch, is the most important hyper-parameter as it explicitly exploits the memorization effect.

Algorithm 1 Framework of the sample-selection approach (Jiang et al., 2018; Han et al., 2018).

```
1: for $t = 1, \cdots, T$ do
2:     shuffle training set $\mathcal{D}$;
3:     for $n = 1, \cdots, N$ do
4:         draw a mini-batch $\bar{\mathcal{D}}$ from $\mathcal{D}$;
5:         select $\bar{\mathcal{D}}_f$, i.e., $R(t)$ small-loss instances from $\bar{\mathcal{D}}$ based on network's predictions;
6:         update the network's parameter using gradient from $\bar{\mathcal{D}}_f$;
7:     end for
8:     update $R(t)$ (estimation on percentage of clean instances);
9: end for
```

However, it is hard to exactly determine *how much* proportion of small-loss samples should be selected in each epoch (Jiang et al., 2018; Ren et al., 2018). As will be discussed in Section 3.1, due to various practical usages issues, to which extend memorization effect can happen is hard to quantize. Thus, performance obtained from existing solutions are far from desired, and we are motivated to solve this issue by AutoML.

2.2 AUTOMATED MACHINE LEARNING (AUTOML)

Automated machine learning (AutoML) (Hutter et al., 2018) has recently exhibited its power in easing the usage of and designing better machine learning models. Basically, AutoML can be regarded as a black-box optimization problem where we need to efficiently and effectively search for hyper-parameters or designs for the underlying learning models evaluated by the validation set.

Regarding the success of AutoML, there are two important perspectives (Feurer et al., 2015; Zoph & Le, 2017; Xie & Yuille, 2017; Bender et al., 2018): 1). *Search space*: Search space is domain-specific. First, it needs to be general enough, which means it should cover existing models as special cases. This also helps experts better understand limitations of existing models and thus facilitate future researches. However, the space cannot be too general, otherwise searching in such a space will be too expensive. 2). *Search algorithm*: Optimization problems in AutoML are usually black-box. Unlike convex optimization, there is no universal and efficient optimization tools. Once the search space is determined, domain knowledge should also be explored in the design of search algorithm so that good candidates in the space can be identified efficiently.

There are two types of search algorithms popularly used in the literature of AutoML. The first one is derivative-free optimization methods, it is usually used for searching in a general search space, e.g., reinforcement learning (Zoph & Le, 2017; Baker et al., 2017), genetic programming (Escalante et al., 2009; Xie & Yuille, 2017), and Bayes optimization (Feurer et al., 2015; Snoek et al., 2012). More recently, one-shot gradient-based methods, which alternatively update parameters and hyper-parameters, have been developed as more efficient replacements for derivative-free optimization methods on some domain-specific search spaces, e.g., the supernet in neural network architecture search (Bender et al., 2018; Liu et al., 2019; Akimoto et al., 2019; Xie et al., 2018). These methods have two critical requirements, i.e., gradients w.r.t hyper-parameters can be computed and parameters can be shared among different hyper-parameters.

3 The Proposed Method

Here, we first give a closer look at why it is difficult to exploit the memorization effect (Section 3.1). This also helps us identify key observations on how memorization can happen. This observation subsequently enables us to design an expressive but compact search space (Section 3.2), and motivates us to use natural gradient method (Amari, 1998; Ollivier et al., 2017) that can generate gradients in the parameterized space for efficient optimization (Section 3.3).

3.1 Key Observations

As in Section 2.2, an important challenge in designing search spaces is to balance the size (or dimension) and the expressive ability of the search space. An overly constrained search space may not contain candidates that have a satisfying performance, whereas too large search spaces will be difficult to effectively search. All these require us to have an in-depth understanding of memorization effect. Thus, we are motivated to look at factors which can affect memorization in practical usages of deep networks, and to seek patterns from the resultant influences. Specifically, we examine memorization when data sets, architectures, or optimizers are changed. Results are in Figure 1. From these figures, we can observe:

- *Foot-stone of space design*: There exists a general pattern among all cases, i.e., all models' test accuracy will first increase, then decrease.

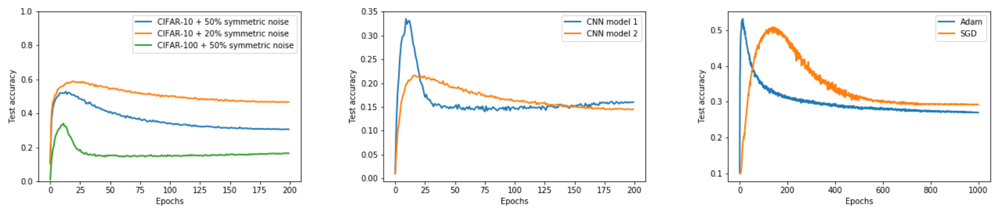

(a) data sets. (b) architectures. (c) optimizers.

Figure 1: Examples of possible factors which can significantly affect the memorization effect (details of experiment are in Appendix A.1).

This general pattern is consistent with that in the literature (Zhang et al., 2016; Arpit et al., 2017; Tanaka et al., 2018; Han et al., 2018). It is also the key domain knowledge for designing an expressive and compact search space, which makes the subsequent search possible. However, the more important observation is:

- *Need of AutoML*: Curvature can be significantly affected by these factors. When the peak will appear (i.e., stop learning from simple patterns and start to over-fit), and to which extend the performance will drop from peak (i.e., over-fit on noisy labels) are all hard to quantize.

This observation shows a great variety in appearances of the memorization effect, which further poses a significant need for automated exploiting of such effect. Besides, it is hard to know in advance what learning curve will exactly look like in advance and thus impossible to manually design before learning is performed.

3.2 Search Space

Recall that in step 8 of Algorithm 1, $R(t)$ controls how many instances are kept in each mini-batch, and we want to exploit the memorization effect through the variation of $R(t)$. Based on the first empirical observation in Section 3.1, our design of $R(t)$ first should satisfy:

- *Curvature*: $R(t)$ should be similar with the inverse of the learning curve. In other words, $R(t)$ should first drop, then (possibly) rise.

The reason behind this constraint is as follows: Since the learning curve represents the model's accuracy, when it rises, we should drop more large-loss samples as the large loss is more likely the result of corrupted labels than model's misclassification. And when the learning curve falls, we should drop less to help the model learn more.

- *Range*: $R(t) \in [0, 1]$ for $t \in \{1, \ldots, T\}$ with $R(1) = 1$.

Since $R(t)$ denotes the proportion of selected instances, it is naturally in $[0, 1]$. Besides, at the beginning, dropping small-loss samples will be same as dropping samples randomly, and we need to pass sufficient number of instances such that the model can learn from patterns.

function	definition
pow$_1$	${}^{1}\!/_{(1+bt)^a}$
exp$_1$	e^{-bt^a}
log	${}^{\log(b)}\!/_{\log(at+b)}$
vapor	$(\frac{t}{t_m})^n e^{1/(1+bt)^a - 1/(1+bt_m)^a}$
exp$_2$	$e^{-b_1 t^{a_1}} + b_2(\frac{t}{t_m})^{a_2}$
pow$_2$	$\frac{1}{(1+b_1 t)^{a_1}} + \frac{\log(1+t^{a_2})}{\log(1+{t_m}^{a_2})} b_2$

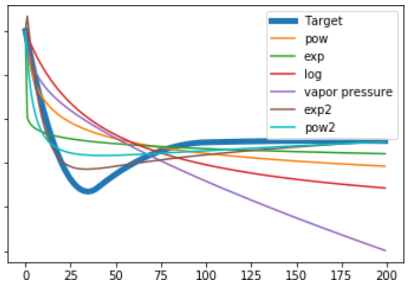

Figure 2: Different candidates for f_i (cf. left table) and their example curvatures (cf. right figure). Target is the assumed ground-truth $R(t)$ we want to approximate.

As $R(t)$ itself can be seen as a function which takes t as input and outputs a scalar, we take "searching for proper $R(t)$" as a function approximation problem. Motivated by the Taylor expansion in calculus (Tao, 2006), which tries to approximate a smooth function with many basis functions, we represent $R(t)$ as a linear combination of a series of functions, i.e.,

$$R(t) = \sum\nolimits_{i=1}^{k} \alpha_i f_i(t), \text{ s.t. } \boldsymbol{\alpha} \in \mathcal{A}, \tag{1}$$

where α_is are hyper-parameter to be determined, $\mathcal{A} \equiv \{\boldsymbol{\alpha} \mid \alpha_i \geq 0, \sum_{i=1}^{k} \alpha_i = 1\}$, and each f_i is a basis function. Note that the sparse constraint $\mathcal{A}$ implies that each f_i should meet above two requirements. There are many candidates which can be used as f_is. Some examples are given in Figure 2, which are previously used in learning curve prediction (Domhan et al., 2015) or as a sparse regularizer (Yao & Kwok, 2017). We note that no single f_i can describe all possibilities of $R(t)$, which is another motivation to use a linear combination of them.

Let the clean validation set be $\mathcal{G}_{val}$, F be Algorithm 1 with network parameter $\boldsymbol{w}$ and sampling rule $\boldsymbol{\alpha}$ ($R(t)$ is parameterized by equation 1). $\mathcal{M}(\boldsymbol{w}, \mathcal{G}_{val})$ measures the validation performance with the model parameter $\boldsymbol{w}$. Thus, memorization effect can be automatically exploited by solving the following problem

$$\boldsymbol{\alpha}^* = \arg\max_{\boldsymbol{\alpha} \in \mathcal{A}} \mathcal{M}\left(\boldsymbol{w}^*(\boldsymbol{\alpha}), \mathcal{G}_{val}\right), \text{ s.t. } \boldsymbol{w}^*(\boldsymbol{\alpha}) = \arg\min_{\boldsymbol{w}} F(\boldsymbol{w}; \boldsymbol{\alpha}). \tag{2}$$

Then, the optimal curvature is derived from $R(t) = \sum_{i=1}^{k} \alpha_i^* f_i(t)$.

Remark 3.1. *In the original Co-teaching algorithm (Han et al., 2018), $R(t)$ is determined as follows*

$$R(t) = 1 - \tau \cdot \min\left(({}^{t}\!/_{t_k})^c, 1\right), \tag{3}$$

which contains three hyper-parameters: τ, c and t_k. Thus, we can formulate a search space as: $\tau \in (0, 1), c \in (0, +\infty)$ and $t_k \in \{1, \cdots, T\}$. The expressivity of such $R(t)$ is not enough as equation 1 here (since equation 3 is covered as a special case).

3.3 Search Algorithm

Here, we first discuss problems of using one-shot gradient-based methods here (Section 3.3.1). These problems motivate us design an efficient search algorithm based on natural gradient algorithm (Section 3.3.2).

3.3.1 ISSUES OF EXISTING ALGORITHMS

Gradient-based methods need the chain rule to obtain the gradient w.r.t hyper-parameters from the gradient w.r.t network weights, i.e., $\nabla_{\boldsymbol{\alpha}}\mathcal{M} = \partial\mathcal{M}/\partial\boldsymbol{w} \cdot \partial\boldsymbol{w}/\partial\boldsymbol{\alpha}$. This condition does not hold for our problem since our hyper-parameters control *how many* samples will be used to update the weights. Thus, it is hard to compute $\nabla_{\boldsymbol{\alpha}}\mathcal{M}$ here. Besides, the learned parameters $\boldsymbol{w}$ cannot be shared among different $\boldsymbol{\alpha}$. In previous methods, hyper-parameters are not coupled with the training process, e.g., network architectures (Liu et al., 2019; Akimoto et al., 2019) and regularization (Luketina et al., 2016). However, $R(t)$ here will heavily influence the training process, which is also shown in our Figure 1. Thus, one-shot gradient-based methods cannot be applied here.

3.3.2 PROPOSED ALGORITHM

The analysis above demonstrates that only derivative-free methods are applicable to our problem, which can be slow. Here, we discover that natural gradient (NG) (Amari, 1998; Pascanu & Bengio, 2013; Ollivier et al., 2017), can be used. The most interesting point here is that NG can still benefit from gradient descent, but without the computation of $\partial\mathcal{M}/\partial\boldsymbol{\alpha}$ or sharing of $\boldsymbol{w}$.

The basic idea of NG is summarized as follows: instead of directly optimizing w.r.t $\boldsymbol{\alpha}$, we consider a random distribution $p_\theta(\boldsymbol{\alpha})$ over $\boldsymbol{\alpha}$ parametrized by θ, and maximize the expected value of our validation performance $\mathcal{M}$ w.r.t θ, i.e.,

$$\max_{\boldsymbol{\theta}} \mathcal{J}(\boldsymbol{\theta}) \equiv \int_{\boldsymbol{\alpha}\in\mathcal{A}} \mathcal{M}\left(\boldsymbol{w}^*(\boldsymbol{\alpha}), \mathcal{G}_{val}\right) p_{\boldsymbol{\theta}}(\boldsymbol{\alpha})\, d\boldsymbol{\alpha}, \text{ s.t. } \boldsymbol{w}^*(\boldsymbol{\alpha}) = \arg\min_{\boldsymbol{w}} F(\boldsymbol{w}; \boldsymbol{\alpha}). \tag{4}$$

To optimize $\mathcal{J}(\boldsymbol{\theta})$ w.r.t $\boldsymbol{\theta}$, NG updates $\boldsymbol{\theta}$ by

$$\boldsymbol{\theta}^{m+1} = \boldsymbol{\theta}^m + \rho \boldsymbol{H}^{-1}(\boldsymbol{\theta}^m)\nabla_{\boldsymbol{\theta}}\mathcal{J}(\boldsymbol{\theta}^m), \tag{5}$$

where ρ is the step-size, $\boldsymbol{H}(\boldsymbol{\theta}^m)$ is the Fisher information matrix at $\boldsymbol{\theta}^m$, and

$$\nabla_{\boldsymbol{\theta}}\mathcal{J}(\boldsymbol{\theta}) = \int_{\boldsymbol{\alpha}\in\mathcal{A}} \mathcal{M}\left(\boldsymbol{w}^*(\boldsymbol{\alpha}), \mathcal{G}_{val}\right) d\boldsymbol{\alpha} = \mathbb{E}_{p_{\boldsymbol{\theta}}(\boldsymbol{\alpha})}\left[\mathcal{M}\left(\boldsymbol{w}^*(\boldsymbol{\alpha}), \mathcal{G}_{val}\right) \nabla_{\boldsymbol{\theta}} \log p_{\boldsymbol{\theta}}(\boldsymbol{\alpha})\right]. \tag{6}$$

First, parameters are not shared between $\boldsymbol{\alpha}$'s as $\boldsymbol{w}$ is obtained from full model trained in equation 4. Second, by sampling candidate $R(t)$s from the given distribution $p_{\boldsymbol{\theta}^m}$ in each iteration, equation 6 just needs validation's performance (without computation of $\partial\mathcal{M}/\partial\boldsymbol{\alpha}$). Besides, such gradient has proved to give the steepest ascend direction in the probabilistic space spanned by $p_{\boldsymbol{\theta}}$ (Theorem 1 in (Angluin & Laird, 1988)).

The last question is how to choose $p_{\boldsymbol{\theta}}$, which may significantly influence the algorithm's convergence behavior. Fortunately, NG exhibits strong robustness against different choices over $p_{\boldsymbol{\theta}}$. The reason is that Fisher matrix, which encodes the second order approximation to the Kullback-Leibler divergence, can accurately capture curvatures introduced by various $p_{\boldsymbol{\theta}}$. Thus, NG descent is parameterization-invariant, has good generalization ability, and moreover can be regarded as a second-order method in the space of $\boldsymbol{\theta}$ (Ollivier et al., 2017). The proposed search algorithm is in Algorithm 2 (details are in Appendix A.2). As will be shown in experiments, all these properties make NG an ideal search algorithm here, and can be faster than other popular AutoML approaches.

Algorithm 2 Proposed search algorithm (based on natural gradient).

```
1: while not converged do
2:     for $n = 1, \cdots, N$ do
3:         draw an $\boldsymbol{\alpha}$ from the current distribution $p_{\boldsymbol{\theta}}(\boldsymbol{\alpha})$;    // approximate gradients
4:         run Algorithm 1 using $R(t)$ described by equation 1;    // no weight-sharing
5:     end for
6:     use samples in step 2-5 to compute Fisher information matrix;
7:     update $\boldsymbol{\theta}$ by equation 5 and 6;
8: end while
```

4 EXPERIMENTS

We implement all our experiments using PyTorch 0.4.1 on a GTX 1080 Ti GPU.

4.1 Experiments on synthetic data

In this section, we demonstrate the superiority of the proposed search space and search algorithm on the synthetic data. The ground-truth $R(t)$ is shown in Figure 3(a), which is an example curvature satisfying two requirements in Section 3.2.

4.1.1 Search space comparison

The goal here is to approximate $R(t)$ in Figure 3(a). Let the estimated function be $\bar{R}(t)$ where $t = 1, \cdots, 200$. The target is to minimize RMSE, i.e., $f(\bar{R}) = [{}^1\!/_{200} \sum_{t=1}^{200} (R(t) - \bar{R}(t))^2]^{1/2}$. Three different search spaces are compared: 1). *Full space*: $\bar{R}_1(t) = \{e_1, \cdots, e_{200}\}$, i.e., there is no constraint in the space, and estimation for $R(t)$ at each time stamp is performed independently; 2). *Co-teaching*'s space in equation 3, i.e., $R_2(t) = 1 - \tau \min(({}^t\!/_{t_k})^c, 1)$, and $\{\tau, c, t_k\}$ needs to be estimated; and 3). The *proposed* space in equation 1, which encodes our observations in Section 3.1. Random search (Bergstra & Bengio, 2012) is performed in all three spaces.

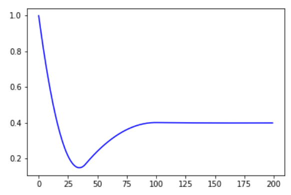

(a) Grount-truth $R(t)$.

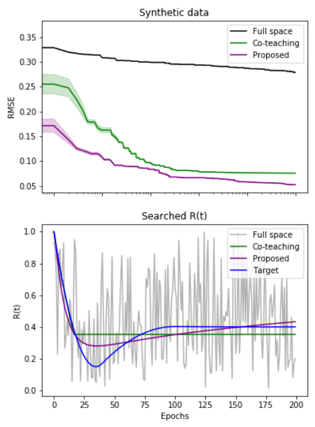

(b) Search space.

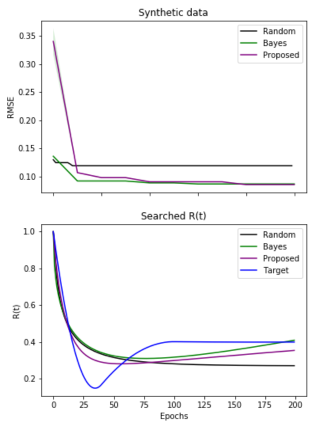

(c) Search algorithm.

Figure 3: Comparison of the search space (cf. the middle figure) and search algorithm (cf. the right figure) on the synthetic data.

Results are in Figure 3(b). We can see that no constraints on the search space will lead to disastrous performance and extremely slow convergence rate. And compare our space with previous Co-teaching's space, we can see that our space can approximate the target better due to its larger degree of freedom.

4.1.2 Search algorithm comparison

We first test our proposed method's efficiency over other hyper-parameter optimization (HPO) algorithms on a synthetic problem as follows: Given a pre-defined $R(t)$ as target, we try to search for a $R(t)$ that has the lowest squared loss to the target. We compare our proposed method with *random search* (Bergstra & Bengio, 2012) and *Bayesian optimization* (Kandasamy et al., 2019), which are two popular methods for hyper-parameter optimization. Results are in Figure 3(c). The results demonstrate that our proposed natural gradient approach has the fastest convergence rate. And it can find the best $R(t)$ with the least RMSE to the target.

4.2 Experiments on benchmark data sets

We verify the efficiency of our approach on three benchmark data sets, i.e., MNIST, CIFAR-10 and CIFAR-100 (details are in Appendix A.3). These data sets are popularly used for the evaluation of learning with noisy labels in the literature (Zhang et al., 2016; Arpit et al., 2017; Jiang et al., 2018; Han et al., 2018). Following (Patrini et al., 2017; Han et al., 2018; Chen et al., 2019), we corrupt these data sets manually by two types of noise. (1) Symmetry flipping (with 20% and 50% noise level): Parts of correct labels are flip uniform randomly to other classes; (2) Pair flipping (with 45% noise level): A simulation of fine-grained classification with noisy labels, where labelers may make mistakes only within very similar classes.

We set the network architecture as the same in (Yu et al., 2019) (Appendix A.4). To measure the performance, same as (Patrini et al., 2017; Han et al., 2018; Chen et al., 2019), we use the test accuracy, i.e., $test\ accuracy = (\#of\ correct\ predictions)/(\#of\ test\ dataset)$. Intuitively, higher test accuracy means that the algorithm is more robust to the label noise.

4.2.1 Comparison on Learning Performance

To show better accuracy can be achieved by automatically exploiting the memorization effect, we compared the proposed method with 1). *MentorNet* (Jiang et al., 2018); 2). *Co-teaching* (Han et al., 2018); 3). *Co-teaching+* (Yu et al., 2019) (enhancing Co-teaching by disagreements on predictions); 4). *Decoupling* (Malach & Shalev-Shwartz, 2017); 5). *F-correction* (Patrini et al., 2017); 6). As a simple baseline, we also compare with the standard deep network that directly trains on noisy datasets (abbreviated as *Standard*). As an example usage, the proposed method is combined with Co-teaching, i.e., Co-teaching is run with search $R(t)$. Figure 4 shows the comparison with various human-designed methods. We can see that the proposed method significantly outperforms existing methods by a large margin, especially on the more noisy cases (i.e., symmetric-50% and pair-45%). Besides, the proposed method not only beats Co-teaching due to better exploiting of the memorization effect, but also wins Co-teaching+, which further filter small-loss instances in Co-teaching by checking disagreements on predictions of labels. These demonstrates the importance and benefits of searching proper $R(t)$.

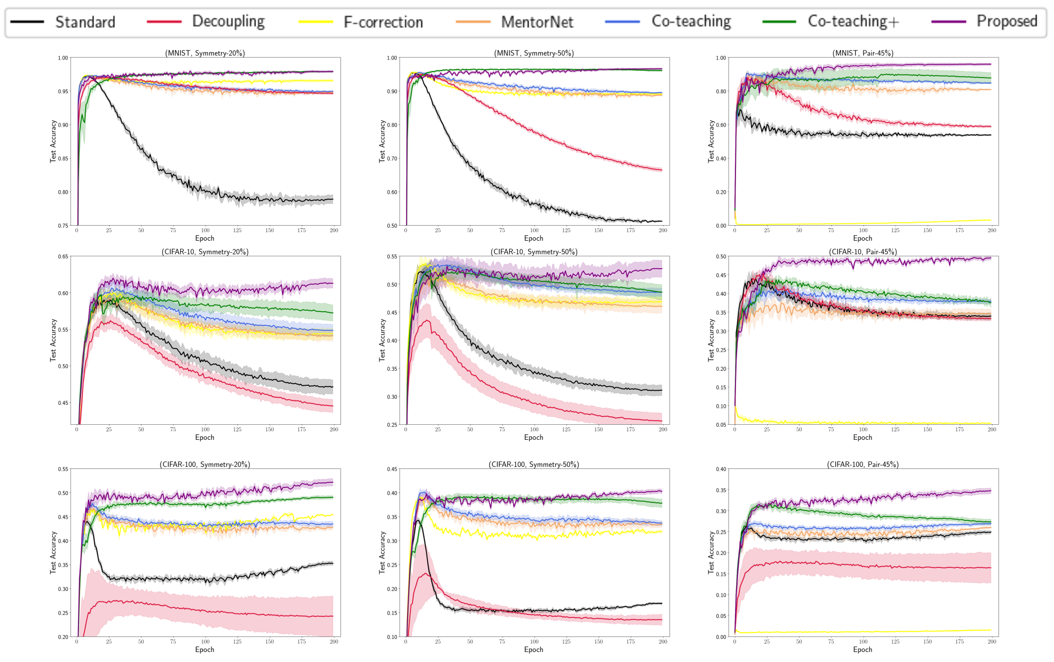

(a) Symmetric 20%. (b) Symmetric 50%. (c) Pair 45%.

Figure 4: Comparison on testing accuracy between the proposed and other human-designed methods. Top to bottom: MNIST, CIFAR-10 and CIFAR-100.

4.2.2 Case Study on Sampling Rate

To understand why the proposed method can obtain much higher testing accuracy, we plot searched $R(t)$ in Figure 5. We can see that all methods finally drop more large-loss instances than the ground-truth noisy level. The reason is very intuitive, a large-loss instance usually also has larger gradient, and it can have much more influences than several clean small-loss instances if its label is wrong. Thus, we may want to drop more samples eventually. However, this is not an easy task, as in Table 8 of (Han et al., 2018), simply making τ larger can significantly decrease testing accuracy. The searched curvature from equation 3 is of great importance. Another interesting observation is that the non-monotonous property of $R(t)$ allowed in Section 3.2 is not useful. This might be due to monotonous curves can already balance well learning and over-fitting here.

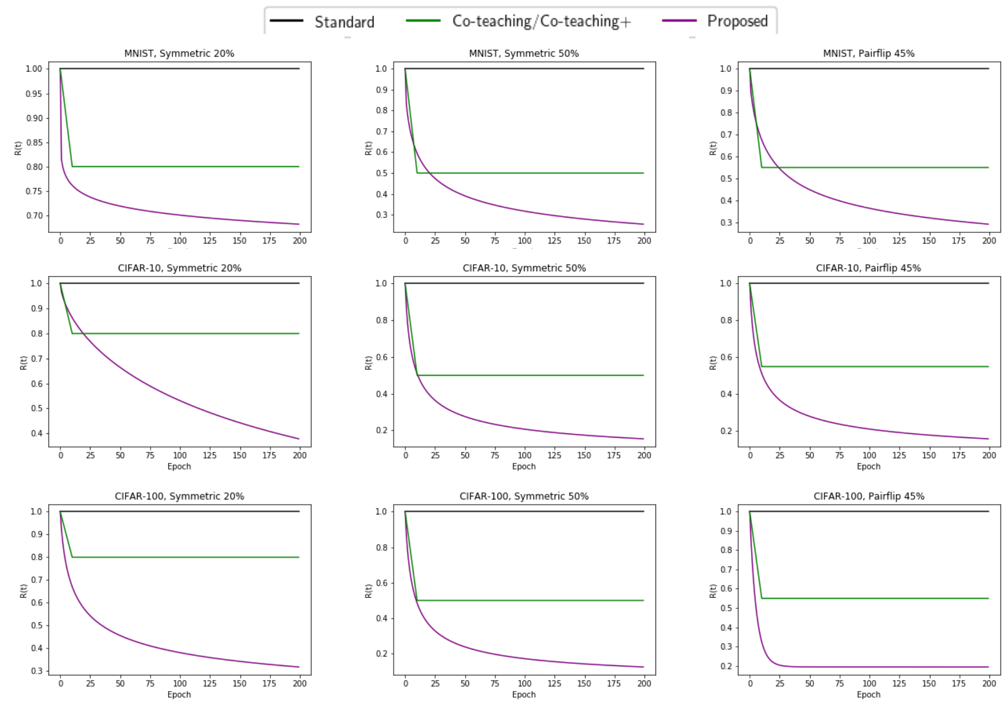

(a) Symmetric 20%. (b) Symmetric 50%. (c) Pair 45%.

Figure 5: Comparison on $R(t)$ between the proposed (automatically searched from the data) and Co-teaching (note that Co-teaching+ uses the same $R(t)$ as Co-teaching). Top to bottom: MNIST, CIFAR-10 and CIFAR-100.

4.3 Comparison with HPO methods

Finally, in this section, we compare the proposed natural gradient (NG) algorithm with 1). *random search* (Bergstra & Bengio, 2012) and 2). *Hyperband* (Li et al., 2017a). Note that Bayesian optimization is slower than *Hyperband*, thus not compared (*Hyperband* cannot be used in Section 4.1.2 due to no inner loops). Besides, reinforcement learning (RL) (Zoph & Le, 2017) is not compared as the searching problem is not a multi-step one. Genetic programming (Xie & Yuille, 2017) is not considered neither, as the search space is a continuous one. Figure 6 compares the proposed method with random search and Hyperband. From the figure, we can see that natural gradient converges faster than other HPO methods in this problem. Our proposed method can also find better $R(t)$s under different data sets and noise settings.

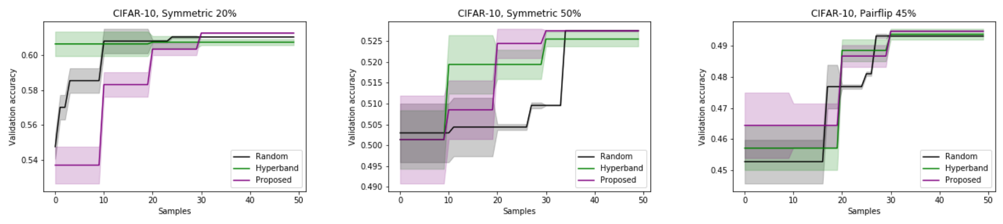

(a) Symmetric 20%. (b) Symmetric 50%. (c) Pair 45%.

Figure 6: Comparison between the proposed search and other HPO algorithm. CIFAR-10 is used.

5 Conclusion

In this paper, motivated by the main difficulty that to what extent the memorization effect of deep networks can happen, we propose to exploit memorization by automated machine learning (AutoML) techniques. This is done by first designing an expressive but compact search space, which is based on observed general patterns for memorization, and designing a natural gradient-based search algorithm, which overcomes the problem of non-differential and failure of parameter-sharing. Extensive experiments on both synthetic data sets and benchmark data sets demonstrate that the proposed method can not only be much efficient than existing AutoML algorithms, but also achieve much better performance than the state-of-the-art sample-selection approach.

REFERENCES

Y. Akimoto, S. Shirakawa, N. Yoshinari, K. Uchida, S. Saito, and K. Nishida. Adaptive stochastic natural gradient method for one-shot neural architecture search. In *ICML*, pp. 171–180, 2019.

S. Amari. Natural gradient works efficiently in learning. *Neural Computation*, 10(2):251–276, 1998.

D. Angluin and P. Laird. Learning from noisy examples. *Machine Learning*, 2(4):343–370, 1988.

D. Arpit, S. Jastrzkbski, N. Ballas, D. Krueger, E. Bengio, M. Kanwal, T. Maharaj, A. Fischer, A. Courville, and Y. Bengio. A closer look at memorization in deep networks. In *ICML*, pp. 233–242. JMLR. org, 2017.

B. Baker, O. Gupta, N. Naik, and R. Raskar. Designing neural network architectures using reinforcement learning. In *ICLR*, 2017.

G. Bender, P.-J. Kinderm, B. Zoph, V. Vasudevan, and Q. Le. Understanding and simplifying one-shot architecture search. In *ICML*, pp. 549–558, 2018.

Y. Bengio, J. Louradour, R. Collobert, and J. Weston. Curriculum learning. In *ICML*, pp. 41–48. ACM, 2009.

J. Bergstra and Y. Bengio. Random search for hyper-parameter optimization. *JMLR*, 13(Feb):281–305, 2012.

P. Chen, B. Liao, G. Chen, and S. Zhang. Understanding and utilizing deep neural networks trained with noisy labels. In *ICML*, pp. 1062–1070, 2019.

T. Domhan, J. Springenberg, and F. Hutter. Speeding up automatic hyperparameter optimization of deep neural networks by extrapolation of learning curves. In *IJCAI*, 2015.

J. Escalante, M. Montes, and Luis E. Sucar. Particle swarm model selection. *JMLR*, 10(Feb):405–440, 2009.

M. Feurer, A. Klein, K. Eggensperger, J. Springenberg, M. Blum, and F. Hutter. Efficient and robust automated machine learning. In *NeurIPS*, pp. 2962–2970, 2015.

A. Ghosh, H. Kumar, and P. Sastry. Robust loss functions under label noise for deep neural networks. In *AAAI*, pp. 1919–1925, 2017.

I. Goodfellow, Y. Bengio, and A. Courville. *Deep learning*. MIT press, 2016.

B. Han, Q. Yao, X. Yu, G. Niu, M. Xu, W. Hu, I. Tsang, and M. Sugiyama. Co-teaching: Robust training of deep neural networks with extremely noisy labels. In *NeurIPS*, pp. 8527–8537, 2018.

F. Hutter, L. Kotthoff, and J. Vanschoren (eds.). *Automated Machine Learning: Methods, Systems, Challenges*. Springer, 2018. In press, available at http://automl.org/book.

L. Jiang, Z. Zhou, T. Leung, L. Li, and L. Fei-Fei. Mentornet: Learning data-driven curriculum for very deep neural networks on corrupted labels. In *ICML*, pp. 2309–2318, 2018.

K. Kandasamy, K. Vysyaraju, W. Neiswanger, B. Paria, C. Collins, J. Schneider, B. Poczos, and E. Xing. Tuning hyperparameters without grad students: Scalable and robust bayesian optimisation with Dragonfly. Technical report, arXiv preprint arXiv:1903.06694, 2019.

Diederik P Kingma and Jimmy Ba. Adam: A method for stochastic optimization. *arXiv preprint arXiv:1412.6980*, 2014.

S. Laine and T. Aila. Temporal ensembling for semi-supervised learning. In *ICLR*, 2017.

L. Li, K. Jamieson, G. DeSalvo, A. Rostamizadeh, and A. Talwalkar. Hyperband: a novel bandit-based approach to hyperparameter optimization. *JMLR*, 18(1):6765–6816, 2017a.

Y. Li, J. Yang, Y. Song, L. Cao, J. Luo, and L.-J. Li. Learning from noisy labels with distillation. In *ICCV*, pp. 1910–1918, 2017b.

H. Liu, K. Simonyan, and Y. Yang. DARTS: Differentiable architecture search. In *ICLR*, 2019.

J. Luketina, M. Berglund, K. Greff, and T. Raiko. Scalable gradient-based tuning of continuous regularization hyperparameters. In *ICML*, pp. 2952–2960, 2016.

X. Ma, Y. Wang, M. Houle, S. Zhou, S. Erfani, S.-T. Xia, S. Wijewickrema, and J. Bailey. Dimensionality-driven learning with noisy labels. In *ICML*, pp. 3361–3370, 2018.

E. Malach and S. Shalev-Shwartz. Decoupling" when to update" from" how to update". In *NIPS*, pp. 960–970, 2017.

T. Miyato, S. Maeda, M. Koyama, and S. Ishii. Virtual adversarial training: A regularization method for supervised and semi-supervised learning. In *ICLR*, 2016.

Y. Ollivier, L. Arnold, A. Auger, and N. Hansen. Information-geometric optimization algorithms: A unifying picture via invariance principles. *JMLR*, 18(1):564–628, 2017.

R. Pascanu and Y. Bengio. Revisiting natural gradient for deep networks. Technical report, arXiv preprint arXiv:1301.3584, 2013.

G. Patrini, A. Rozza, A. Menon, R. Nock, and L. Qu. Making deep neural networks robust to label noise: a loss correction approach. In *CVPR*, pp. 2233–2241, 2017.

S. Reed, H. Lee, D. Anguelov, C. Szegedy, D. Erhan, and A. Rabinovich. Training deep neural networks on noisy labels with bootstrapping. In *ICLR Workshop*, 2015.

M. Ren, W. Zeng, B. Yang, and R. Urtasun. Learning to reweight examples for robust deep learning. In *ICML*, pp. 4331–4340, 2018.

J. Snoek, H. Larochelle, and R. Adams. Practical Bayesian optimization of machine learning algorithms. In *NIPS*, pp. 2951–2959, 2012.

S. Sukhbaatar, J. Bruna, M. Paluri, L. Bourdev, and R. Fergus. Training convolutional networks with noisy labels. In *ICLR Workshop*, 2015.

D. Tanaka, D. Ikami, T. Yamasaki, and K. Aizawa. Joint optimization framework for learning with noisy labels. In *CVPR*, pp. 5552–5560, 2018.

Terence Tao. *Analysis*, volume 1. Springer, 2006.

A. Tarvainen and H. Valpola. Mean teachers are better role models: Weight-averaged consistency targets improve semi-supervised deep learning results. In *NIPS*, 2017.

L. Xie and A. Yuille. Genetic CNN. In *ICCV*, pp. 1388–1397, 2017.

S. Xie, H. Zheng, C. Li, and L. Lin. SNAS: stochastic neural architecture search. In *ICLR*, 2018.

Q. Yao and J. Kwok. Efficient learning with a family of nonconvex regularizers by redistributing nonconvexity. *JMLR*, 18:179–1, 2017.

X. Yu, B. Han, J. Yao, G. Niu, I. Tsang, and M. Sugiyama. How does disagreement help generalization against label corruption? In *ICML*, pp. 7164–7173, 2019.

C. Zhang, S. Bengio, M. Hardt, B. Recht, and O. Vinyals. Understanding deep learning requires rethinking generalization. *ICLR*, 2016.

B. Zoph and Q. Le. Neural architecture search with reinforcement learning. In *ICLR*, 2017.

A Implementation Details

A.1 Details for Figure 1

We use the same CIFAR-10/100 datasets below. The number of training epochs is 200 for Figure 1(a)(b) and 1000 for Figure 1(c). The CNN model 1 in Figure 1(b) is the same as the CNN model used for CIFAR-100 while the CNN model 2 is the same as that used for CIFAR-10. In Figure 1(c), the initial learning rate for the Adam optimizer is 0.001 and it is linearly decayed to zero from the 80th epoch to final. The initial learning rate for the SGD optimizer is 0.1, and decay to 0.01 and 0.001 from the 500th and 750th epoch, respectively. The batch size in all experiments is set to 128.

A.2 Natural Gradient

Since our search space for α is bounded, we use Beta distribution in natural gradients, i.e. $p_\theta(\lambda) = \prod_{i=1}^{k} Beta(\alpha_i; \theta_i)$. Each Beta distribution has two parameters x, y and the probability density function (PDF) is given by $Beta(\alpha; x, y) = \frac{\Gamma(x+y)}{\Gamma(x)+\Gamma(y)} \alpha^{x-1}(1-\alpha)^{y-1}$ where $\Gamma(x)$ is the gamma function. The Fisher information matrix $\boldsymbol{H}(\theta) = \mathbb{E}_{p_\theta(\boldsymbol{\alpha})}\left[\nabla_\theta \log p_\theta(\boldsymbol{\alpha}) \nabla_\theta \log p_\theta(\boldsymbol{\alpha})^T\right]$ is estimated by samples since no explicit formula is available. And the gradient in Fisher $\nabla_\theta \log p_\theta(\boldsymbol{\alpha})$ is different for different parameters x and y, as $\nabla_x \log Beta(\alpha; x, y) = \log(\alpha) + \psi(x+y) - \psi(x)$ and $\nabla_y \log Beta(\alpha; x, y) = \log(1-\alpha) + \psi(x+y) - \psi(y)$, where $\psi(x)$ denotes the digamma function.

For synthetic data, we run for 10 iterations and in each iteration, we sample 10 samples and evaluate its performance. The learning rate for natural gradient is set to 80.

For benchmark data sets, all search algorithms will run for 5 iterations in total. In random search and natural gradient, we sample 20 samples for MNIST and CIFAR-100, and 10 samples for CIFAR-10 to evaluate its performance in each iteration. The learning rate for natural gradient is set to 20, 500, 80 for MNIST, CIFAR-10, CIFAR-100 data set respectively.

To obtain a better estimation of the Fisher information matrix, in spite of those samples for evaluation, we also sample another 10000 samples to compute the Fisher in each iteration.

A.3 Data sets

We obtain all the datasets used in our experiments by PyTorch's torchvision package. Some statistics about those datasets are given below.

Table 1: Summary of data sets used in the experiments.

	# of train	# of validation	# of test	# of class
MNIST	60,000	5,000	5,000	10
CIFAR-10	50,000	5,000	5,000	10
CIFAR-100	50,000	5,000	5,000	100

A.4 Network Structure

Adam optimizer (Kingma & Ba, 2014) (momentum=0.9) is used with an initial learning rate of 0.001, and the batch size is set to 128 and we run 200 epochs. The learning rate is linearly decayed to zero from 80 to 200 epochs.

Table 2: MLP and CNN models used in our experiments.

MLP on MNIST	CNN on CIFAR-10	CNN on CIFAR-100
28×28 Gray Image	32×32 RGB Image	32×32 RGB Image
Dense 28×28→256, ReLU	5×5 Conv, 6 ReLU 2×2 Max-pool	3×3 Conv, 64 BN, ReLU 3×3 Conv, 64 BN, ReLU 2×2 Max-pool
	5×5 Conv, 16 ReLU 2×2 Max-pool	3×3 Conv, 128 BN, ReLU 3×3 Conv, 128 BN, ReLU 2×2 Max-pool
	Dense 16×5×5→120, ReLU Dense 120→84, ReLU	3×3 Conv, 196 BN, ReLU 3×3 Conv, 196 BN, ReLU 2×2 Max-pool
Dense 256→10	Dense 84→10	Dense 256→100

A.5 Details Comparison with Co-teaching+

Table 3: Test accuracy (%) of Co-teaching+ and the proposed method on MNIST/CIFAR-10/CIFAR-100 over last 10 epochs.

		Symmetric 20%	Symmetric 50%	Pairflip 45%
MNIST	Co-teaching+	97.88%±0.08%	96.06%±0.31%	87.76%±3.30%
	Proposed	**97.89%±0.01%**	**96.58%±0.01%**	**95.89%±0.01%**
CIFAR-10	Co-teaching+	57.84%±0.80%	49.24%±1.50%	38.17%±0.73%
	Proposed	**61.16%±0.41%**	**52.75%±0.86%**	**49.48%±0.01%**
CIFAR-100	Co-teaching+	49.09%±0.37%	38.15%±0.80%	27.28%±0.70%
	Proposed	**52.17%±0.46%**	**41.66%±0.01%**	**34.73%±0.01%**